



Depth Profiling of La₂O₃/HfO₂ Stacked Dielectrics for Nanoelectronic Device Applications

H. N. Alshareef,^{a,z} S. Mure,^b P. Majhi,^c and M. A. Quevedo-Lopez^d

^aMaterials Science and Engineering, King Abdullah University of Science and Technology, Thuwal 23955-6900, Saudi Arabia

^bKobe Steel Ltd., Machinery and Engineering Company, Takasago 676-8670, Japan

^cINTEL Assignee to SEMATECH, Austin, Texas 78748, USA

^dMaterials Science and Engineering, University of Texas at Dallas, Richardson, Texas 75080, USA

Nanoscale La₂O₃/HfO₂ dielectric stacks have been studied using high resolution Rutherford backscattering spectrometry. The measured distance of the tail-end of the La signal from the dielectric/Si interface suggests that the origin of the threshold voltage shifts and the carrier mobility degradation may not be the same. Up to 20% drop in mobility and 500 mV shift in threshold voltage was observed as the La signal reached the Si substrate. Possible reasons for these changes are proposed, aided by depth profiling and bonding analysis.

© 2011 The Electrochemical Society. [DOI: 10.1149/1.3526141] All rights reserved.

Manuscript submitted September 2, 2010; revised manuscript received November 19, 2010. Published January 3, 2011.

The efforts to replace polycrystalline silicon transistor gate electrodes with metal gates continue unabated. However, the development of metal gates with effective work functions near the Si band-edges has been difficult on Hf-based gate dielectrics due to Fermi level pinning and/or interfacial dipole formation.^{1,2} Significant activity is therefore taking place to engineer the metal gates/dielectric stacks to achieve the desired band-edge work functions (4.05 eV for n-channel and 5.15 eV for p-channel devices). One approach that has been extensively studied includes using interfacial layers such as Al₂O₃ and La₂O₃, inserted between the metal gate and the Hf-based high-*k* material.³⁻⁹ Additional approaches include using low thermal budget flows,¹⁰ nitrogen control at the interface,¹¹ and metal capping layer for interface oxide control.¹² In this article, we correlate La depth profile, measured with depth resolution as low as 0.2 nm by high resolution Rutherford backscattering spectrometry (HR-RBS), to measure device characteristics in La₂O₃-containing gate stacks.

Lightly doped p-type Si wafers were used for the study. Prior to deposition of the gate stacks, the substrates were thoroughly wet cleaned. The gate stack (La₂O₃/HfO₂) was formed by first depositing 2.0 nm HfO₂ films using atomic layer deposition at 250°C. The HfO₂ films were then annealed at 750°C in NH₃ for 60 s. La₂O₃ (1–2 nm) was then deposited *ex situ* at room temperature by a sputter deposition system equipped with a shield. No SiO₂ layer was intentionally grown in these stacks and any reference to the SiO₂ layer here refers to SiO₂ that normally result from surface cleaning or thermal anneals. The presence of nearly 1.0 nm SiO₂ could be seen using transmission electron microscopy (not shown). Some blanket samples were subsequently annealed at 1000°C, 10 sec to simulate standard junction anneals. Carrier mobility was measured on transistors with identical La₂O₃ thickness as the blanket wafers by using a previously described transistor flow. HR-RBS analysis was performed using a KOBE HR-RBS500 system. A 450 keV beam of He⁺ ions was generated with 25 nA current and a beam size of 1 mm × 1 mm.⁸ A relatively high detection angle (110°) was selected in order to separate La from Hf without compromising depth resolution.

Figure 1 shows the experimental spectra collected from all samples. Each sample was measured with optimized channeling through the Si substrate to maximize depth resolution. More significant changes can be seen in the La signal compared to Hf or oxygen, suggesting that La is the main diffusing species. For example, the 2.0 nm La₂O₃ sample (labeled c in Fig. 1) shows a widening of the La peak after annealing (labeled d), but not the Hf or Si peaks. The inset of Fig. 1 shows the experimental and simulated Rutherford backscattering (RBS) spectra for a 1.0 nm La₂O₃/HfO₂/Si sample.

Note that the simulated spectra fit the experimental data very well, which permits the extraction of depth information with high accuracy. The kink in the Si signal at about 200 channel number is due to channeling through the Si substrate, which was maximized by carefully manipulating the geometry of the setup to improve the depth resolution. Using these spectra, the depth profile for each one of the elements was generated using KOBE's proprietary HR-RBS software. The results of this analysis are shown in Fig. 2 for the 1.0 nm La₂O₃/HfO₂ sample annealed at 1000°C, 10 s. Figure 2 shows that the elemental depth information can be obtained with excellent resolution (resolution is estimated at 0.2 nm at the surface of the stack and degrading to 0.6 nm at a depth of 4 nm for La and Hf). The La atoms that seem to have diffused slightly passed the midpoint of the HfO₂ film. Furthermore, the La profile appears to be uniform in depth, showing an average atomic concentration of roughly 10%. The La signal disappears nearly 0.7 nm away from the Si substrate. In comparison, the 2.0 nm La₂O₃/HfO₂ sample, annealed at 1000°C, 10 s is shown in Fig. 3. The data in Fig. 3 show that the La atoms have diffused completely throughout the HfO₂ film, nearly reaching the Si substrate interface. This sample also shows that the La distribution in the HfO₂ film is rather uniform, with an average 10 atom % concentration. Figure 4 shows the effective mobility curves of n-channel devices of gate stacks containing 0.0, 1.0, and 2.0 nm La₂O₃ annealed at 1000°C, 10 s. These mobilities are an average of at least five curves on each wafer. It is clear from Fig. 4 that a lower carrier mobility is obtained with increased La₂O₃ thickness, where the La atoms diffuse closer to the Si substrate. For the 1.0 and 2.0 nm La₂O₃ stacks, La diffused to about 0.7 nm and essentially 0 nm from the Si substrate surface, respectively; this resulted in 9 and 20% drop, respectively, in mobility compared to samples having no La₂O₃. Similar to published reports, we also observe a transistor threshold voltage shift with La₂O₃ thickness, but this effect seems to quickly saturate (inset of Fig. 4). An interesting observation is that the n-channel transistor mobility varies more strongly with the distance of the tail-end of the La signal from the Si substrate than the threshold voltage. While the threshold voltage shifted by up to 500 mV in total, most of this shift occurred by the time the La₂O₃ thickness is increased to 1.0 nm. The shift in the threshold voltage then slows down varying by only ~40 mV as the La₂O₃ thickness was increased from 1 to 2 nm. In contrast, the mobility degradation nearly doubles (9 vs 20%) as the La₂O₃ thickness increases from 1 to 2 nm.

These results indicate that the origin of the mobility and threshold voltage changes with La₂O₃ cannot be entirely the same. The mobility degradation seems to correlate well with the physical location of the La tail-end in the gate stack, but not the threshold voltage. It is known that the effective mobility of a device (μ_{eff}) is given by Matthiessen's rule, where mobilities are limited by various scat-

^z E-mail: husam.alshareef@kaust.edu.sa

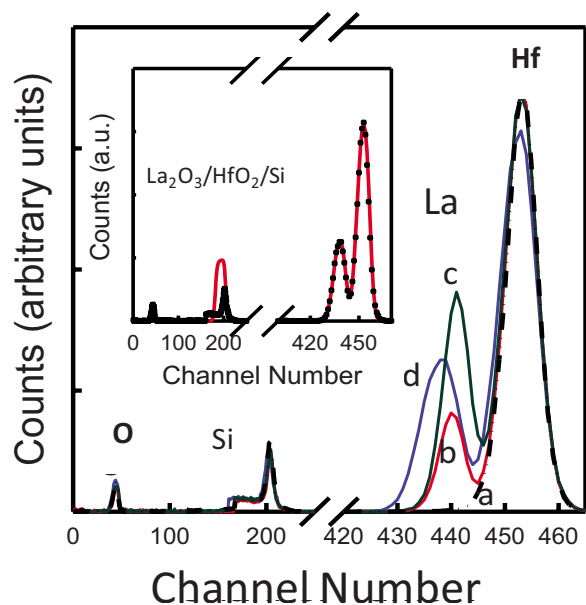


Figure 1. (Color online) Experimental RBS spectra for four different samples with various La_2O_3 thickness or anneal condition. It can be seen that most of the changes in the spectra are due to La interdiffusion. (a) No La_2O_3 , (b) 1.0 nm La_2O_3 plus 1000°C, 10 s anneal, (c) 2.0 nm La_2O_3 but unannealed, and (d) 2.0 nm La_2O_3 plus 1000°C, 10 s anneal. The inset shows that good fits of the experimental data were obtained.

tering mechanisms that add in parallel (columbic, surface roughness, and remote phonon scattering). It is unlikely that the surface roughness is a key contributor to the increased mobility degradation with La_2O_3 thickness. This is because this scattering mechanism becomes important at high electric fields, but the three devices seem to have a similar mobility at high fields. The mobility degradation due to columbic scattering, however, cannot be ruled out. Columbic scattering can result from charges generated by reactions between La_2O_3 and HfO_2 . For example, La^{3+} substitution on Hf^{4+} site can lead to the generation of positively charged oxygen vacancies. While the charges can balance out (i.e., $2\text{La}'_{\text{Hf}} = \text{V}_\text{O}^{\bullet\bullet}$), their physical location

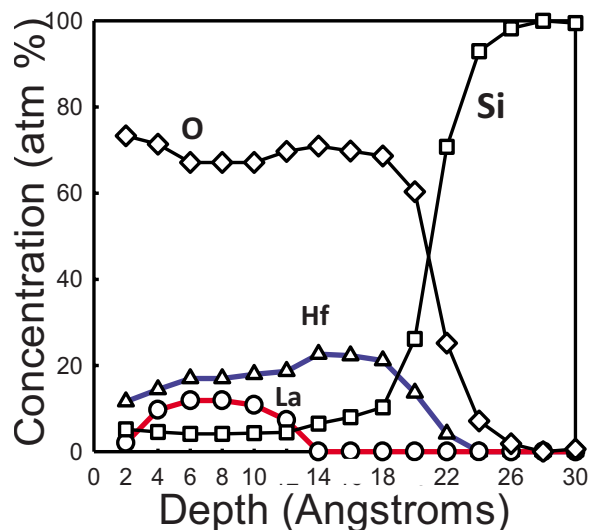


Figure 2. (Color online) Depth profile of a 1.0 nm $\text{La}_2\text{O}_3/\text{HfO}_2$ sample after annealing at 1000°C, 10 s. The profile indicates that for 1.0 nm La_2O_3 , La signal ends 0.7 nm from the interface of the Si substrate after annealing. The average composition of La in the film is around 10 atom %.

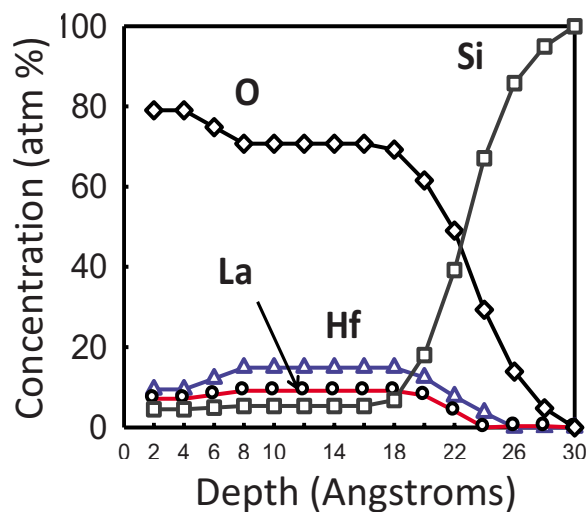


Figure 3. (Color online) Depth profile of a 2.0 nm $\text{La}_2\text{O}_3/\text{HfO}_2$ sample after annealing at 1000°C, 10 s. The profile indicates that in the case of 2.0 nm La_2O_3 , La reaches the Si substrate interface. The average composition of La with depth in the film is about 10 atom %.

relative to the dielectric/Si interface may not be the same, creating an effective charge at some distance from the Si interface into the gate stack. It is likely that such an effective charge can cause the observed mobility degradation via columbic scattering effect, an effect that is expected to increase as La diffuses closer to the Si substrate.

The cause of the threshold voltage shift appears to be different in origin. We noted earlier that the threshold voltage shift saturates quickly where about a 40 mV change in V_t was observed as the La_2O_3 thickness was doubled from 1 to 2 nm. If the threshold voltage shift were primarily caused by fixed charges, we would have observed that V_t continues to shift as the La_2O_3 thickness increased and La diffused closer to the Si substrate. This is not the case, however. It has been proposed that La incorporation in HfO_2/Si gate

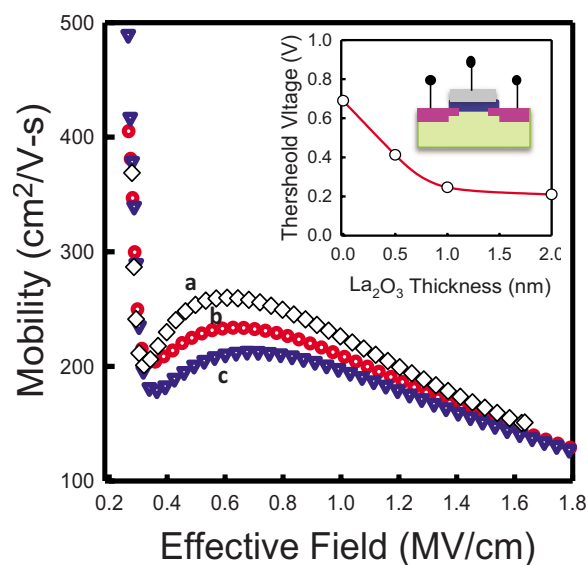


Figure 4. (Color online) Carrier mobility for transistors comprising three different gate stacks: (a) no La_2O_3 , (b) 1.0 nm La_2O_3 , and (c) 2.0 nm La_2O_3 on HfO_2/Si . The mobility degrades with increasing La_2O_3 thickness in correlation with RBS data showing deeper penetration of La after annealing. The inset shows that the transistor threshold voltage simultaneously shifts with increasing La_2O_3 thickness.

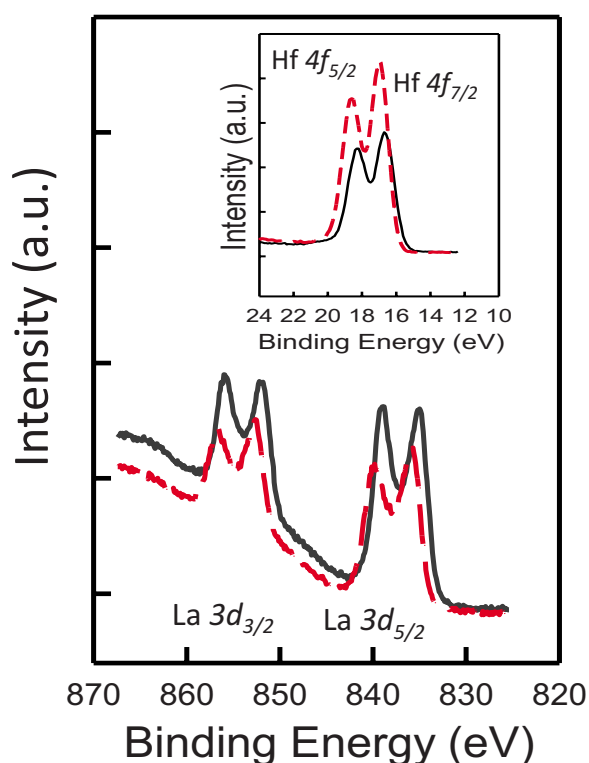


Figure 5. (Color online) XPS results showing that the Hf4f and La3d regions in the case of the 2 nm La_2O_3 sample shift to higher energy after annealing (solid line is before and dotted line is after annealing). This shift was much smaller in the Si2p peaks, suggesting that reactions are mainly taking place between Hf and La oxides.

stacks results in dipole formation that can cause flatband voltage shifts.^{13,14} The prevailing thought appears to be that such dipoles result from bonds having electronegativity differences between metal and oxygen atoms (La–O, Hf–O, Si–O, etc.). The dipole strength can be estimated based on the bond length and the electronegativity difference which is found to increase in strength from La–O > Hf–O > Si–O; this model can predict the direction and magnitude of the threshold voltage shift.¹⁴ Based on the RBS depth profiles and our V_t data, it is seen that the 1.0 nm La_2O_3 sample causes significant V_t shift compared to the reference (no La_2O_3 sample) even though the RBS clearly shows that the La signal is far from the Si substrate surface. The dipoles therefore can be expected to shift the threshold voltage regardless of their location in the gate stack. Thus, it is no surprise that the V_t shift for 1.0 and 2.0 nm La_2O_3 is roughly the same (460 vs 500 mV relative to the reference sample) despite their large mobility difference.

We should pause here and ponder how fixed charges can cause mobility degradation but not so much V_{FB} shift. For one thing, fixed charges can be compensated by other defects (e.g., $2\text{La}'_{\text{Hf}}$ can be compensated by V''_{O}) so that the net effect on V_{FB} is canceled out. In contrast, mobility degradation will occur due to scattering effects regardless of whether the fixed charges are compensated or not. In addition, if we assume all observed V_{FB} shift to be a result from La-induced fixed charges located at the dielectric stack/substrate interface, and knowing that the measured fixed charges in our devices

are 10^{10} – 10^{12} charges/cm², depending on the La_2O_3 thickness, we calculate only a 36 mV shift in V_{FB} in a stack with $Q_f = 1 \times 10^{12}$ charges/cm². However, the observed V_{FB} shift is far larger and is ~ 500 mV. Therefore, we conclude that most of the threshold voltage shift here is likely to be dipole related.

The X-ray photoemission spectroscopy (XPS) results for our samples are shown in Fig. 5, where the La3d and Hf4f doublets for 2 nm $\text{La}_2\text{O}_3/\text{HfO}_2$ stack are shown before and after annealing at 1000°C. It can be seen that both peaks shift to higher energy upon annealing by nearly 0.3 and 0.8 eV for Hf4f and La3d, respectively. The Hf4f peak intensity increased while the La3d intensity drops after annealing. This indicates that La diffuses downward, making it easier to detect Hf4f. In comparison, the Si2p peaks (not shown) in these $\text{La}_2\text{O}_3/\text{HfO}_2$ gate stacks showed a much smaller shift. Similar trends were seen for the 1.0 nm La_2O_3 sample. This clearly indicates that main reactions taking place in these stacks are predominantly a result of the changing bonding environment of the La_2O_3 and HfO_2 , which is consistent with the HR-RBS results. The fact that the Si2p peak (from Si in the interfacial SiO_2 layer) in these samples did not shift much upon annealing may indicate that no significant reaction has taken place between La and any interfacial SiO_2 layer in these samples.

In conclusion, we have used HR-RBS to determine the depth profile of La in $\text{La}_2\text{O}_3/\text{HfO}_2$ gate stacks with excellent depth resolution. The La atoms are the main diffusing species and the physical proximity of the La atoms to the dielectric/Si substrate interface correlates well with the carrier mobility degradation. The mobility degradation is surmised to occur as a result of columbic scattering caused by La diffusion to the interface. The threshold voltage shift is most likely caused by the dipole formation, although a small fixed charge contribution cannot be ruled out.

King Abdullah University of Science and Technology assisted in meeting the publication costs of this article.

References

1. Y.-C. Yeo, T.-J. King, and C. Hu, *J. Appl. Phys.*, **92**, 7266 (2002).
2. J. Tersoff, *Phys. Rev. Lett.*, **52**, 465 (1984).
3. H. N. Alshareef, M. A. Quevedo, H. C. Wen, R. Harris, P. Kirsch, P. Majhi, B. H. Lee, R. Jammy, D. J. Lichtenwalner, J. S. Jur, et al., *Appl. Phys. Lett.*, **89**, 232103 (2006).
4. J.-A. Ng, N. Sugii, K. Kakushima, P. Ahmet, T. Hattori, K. Tsutsui, and H. Iwai, *ECS Trans.*, **2**(1), 329 (2006).
5. P. Ahmeta, K. Nakagawa, K. Kakushimab, H. Nohirac, K. Tsutsuib, N. Sugiib, T. Hattoria, and H. Iwaia, *Microelectron. Reliab.*, **48**, 1769 (2008).
6. S. Kamiyama, T. Miura, E. Kurosawa, M. Kitajima, M. Ootuka, T. Aoyama, and Y. Nara, *Tech. Dig. - Int. Electron Devices Meet.*, **2007**, 539.
7. K. Kakushima, K. Tachib, M. Adachib, K. Okamoto, S. Satob, J. Songb, T. Kawanagob, P. Ahmetb, K. Tsutsuia, N. Sugiia, et al., *Solid-State Electron.*, **54**, 715 (2010).
8. K. Kimura, S. Joumori, Y. Oota, K. Nakajima, and M. Suzuki, *Nucl. Instrum. Methods Phys. Res. B*, **219–220**, 351 (2004).
9. M. Copel, S. Guha, N. Bojarczuk, E. Cartier, V. Narayanan, and V. Paruchuri, *Appl. Phys. Lett.*, **95**, 212903 (2009).
10. L.-A. Ragnarsson, Z. Li, J. Tseng, T. Schram, E. Rohr, M. J. Cho, T. Kauerauf, T. Conard, Y. Okuno, B. Parvais, et al., *Tech. Dig. - Int. Electron Devices Meet.*, **2009**, 663.
11. C. L. Hinkle, R. V. Galatage, R. A. Chapman, E. M. Vogel, H. N. Alshareef, C. Freeman, E. Wimmer, H. Niimi, A. Li-Fatou, J. B. Shaw, et al., *Appl. Phys. Lett.*, **96**, 103502 (2010).
12. H. Takahashi, H. Minakata, Y. Morisaki, S. Xiao, M. Nakabayashi, K. Nishigaya, T. Sakoda, K. Ikeda, H. Morioka, N. Tamura, et al., *Tech. Dig. - Int. Electron Devices Meet.*, **2009**, 427.
13. P. D. Kirsch, P. Sivasubramani, J. Huang, C. D. Young, M. A. Quevedo-Lopez, H. C. Wen, H. Alshareef, K. Choi, C. S. Park, K. Freeman, et al., *Appl. Phys. Lett.*, **92**, 09290 (2008).
14. K. Kakushima, K. Okamoto, M. Adachi, K. Tachi, P. Ahmet, K. Tsutsui, N. Sugii, T. Hattori, and H. Iwai, *Solid-State Electron.*, **52**, 1280 (2008).